Journal Pre-proof

Evaluation of a new inverse, globally convex TPS algorithm for Gamma Knife® radiosurgery within a prospective trial - advantages and disadvantages in practical application

Feline Heinzelmann , Moritz Budde , Irenäus A. Adamietz , Kevin Kröninger , Jan P. Boström

PII: S2452-1094(22)00112-9
DOI: https://doi.org/10.1016/j.adro.2022.101006
Reference: ADRO 101006

To appear in: *Advances in Radiation Oncology*

Received date: 2 March 2022
Accepted date: 25 May 2022

Please cite this article as: Feline Heinzelmann , Moritz Budde , Irenäus A. Adamietz , Kevin Kröninger , Jan P. Boström , Evaluation of a new inverse, globally convex TPS algorithm for Gamma Knife® radiosurgery within a prospective trial - advantages and disadvantages in practical application, *Advances in Radiation Oncology* (2022), doi: https://doi.org/10.1016/j.adro.2022.101006

Evaluation of a new inverse, globally convex TPS algorithm for Gamma Knife® radiosurgery within a prospective trial - advantages and disadvantages in practical application

Inverse treatment planning for Gamma Knife®

Feline Heinzelmann[1], Moritz Budde[3], Irenäus A. Adamietz[2, 3], Kevin Kröninger[1], Jan P. Boström[2, 3]

1. *TU Dortmund University, Department of Physics, Dortmund, Germany*
2. *University Hospital at Ruhr-Universität Bochum, Gamma Knife Zentrum, Bochum, Germany*
3. *Marien Hospital Herne, University Hospital at Ruhr-Universität Bochum, Clinic for Radiotherapy and Radiation Oncology, Herne, Germany*

Corresponding Author:
Feline Heinzelmann: feline.heinzelmann@tu-dortmund.de

Author Responsible for Statistical Analysis:
Feline Heinzelmann: feline.heinzelmann@tu-dortmund.de

Conflict of Interest Statement for All Authors:
Conflict of Interest: None

Funding Statement:
Funding: None.

Data Availability Statement for this Work:
Research data are stored in an institutional repository and will be shared upon request to the corresponding author.

Acknowledgements:
None.

Abstract

Introduction: A new inverse planning (IP) software based on a global convex optimization algorithm was adopted for the Gamma Knife radiosurgery (GKRS). We investigated the IP's suitability for daily clinical use and its applicability for different cerebral entities.

Methods and Materials: For 230 target volumes, IP was tested in a prospective trial. The computed treatment plans were compared with conventional expert pre-plans, which included forward planning by the expert and local internal optimization. Based on the same dose constraints, we used the default settings for the inverse calculation of the treatment plans. Plan quality metrics such as the Paddick conformity index (PCI) were compared for both planning techniques with additional subdivisions into the three selectable IP planning strategies and different entity groups.

Results: IP calculated treatment plans of the quality similar to pre-plans created by expert planners. Some plan quality metrics, especially those related to conformity and dose gradient, attained statistically significant higher scores combined with high coverage for the inversely generated plans except for the selectivity optimizing strategy. Normal Brain ώ. ϱ or ώ ϱ did not show significant differences for the coverage optimizing strategies. IP demonstrated significantly shorter planning times versus manual planning as well as greater numbers of isocenters, often associated with longer treatment times. In terms of total time, these differences almost balanced out again.

Conclusions: Our results suggest that IP is advantageous for complex tumors. We observed general clinical significance for conformity and superiority for the selectivity optimizing strategy. Finally, the high-quality calculation from IP enables the novices in the profession to achieve the treatment of the pre-plan quality. IP allows for optimizing the sparing of surrounding tissue-and the conformity for benign tumors within a short time. Thus, IP forms a solid basis for further planning on the treatment day.

Purpose

In the early 1950s, the Swedish neurosurgeon Lars Leksell introduced stereotactic radiosurgery to treat localized narrow lesions in the brain[1]. Leksell used cross-firing photon beams instead of an open surgery procedure. Recently, the use of Leksellôs approach, known as Gamma Knife® (GK), has considerably increased and has been applied to treat benign and malignant brain tumors, vascular malformations, and functional disorders because of its high dose gradient and high precision[2–4].

In contrast to other radiotherapies, in Gamma Knife® radiosurgery (GKRS), the standard technique for radiation treatment planning is forward planning, which includes the manual placement of isocenters. In the next step, they can be edited through the internal optimization in Leksell GammaPlan® (LGP) software, optimizing the position, weight, and collimator configuration of all the shots in the target according to an objective function. However, this inverse dose planning often finds only the local and not the global minimum of the cost function[5]. In addition, the time for treatment planning depends on the plannerôs experience. Therefore, an alternative or complement is being sought in the form of an automated inverse dose planning, particularly for complex and irregularly shaped target volumes (TVs). The software IntuitivePlan® (IP) with an inverse planning algorithm developed by a university start-up company presents such an alternative. It was CE marked for its use with Leksell Gamma Knife® in June 2019. We have been provided with this algorithm free of charge for study purposes. The software promises to find the global minimum by prescribing a dose to the target volume and specifying dose constraints for the organs at risk (OARs)[5].

The specific objective of this study was to examine the default performance of IP in comparison to the common expert planning technique in clinical routine. We conducted a prospective study with 117 cases of different cerebral diseases using both methods in each case. Further, our research aimed to verify the applicability of IP for various diseases that occurred within the scope of this study.

Methods and Materials

Study assembly

In total, over 100 planning examples with different cerebral diseases treated with GK PerfexionÊ participated in the prospective clinical trial. In the final analysis, the data of a total of 117 treatment cases were evaluated. The treated entities are classified as benign, malignant, functional, and vascular (**Table 1**). Cerebral singular and multiple metastases were counted among malign disorders. Acoustic neuromas (ANs) and other neurinomas, pituitary adenomas, and meningiomas were classed as benign entities, whereas arteriovenous malformations (AVMs), fistulas, and cavernomas were categorized as vascular diseases and trigeminal neuralgias as functional disorders. The contouring of TVs and OARs was performed on T1- and T2-weighted 1-mm thin-layered 3D magnetic resonance imaging (MRI) images by Brainlab® ElementsÊ (Anatomical Mapping 1.1, SmartBrush 3.0).

Table 1 Anonymized for Review.

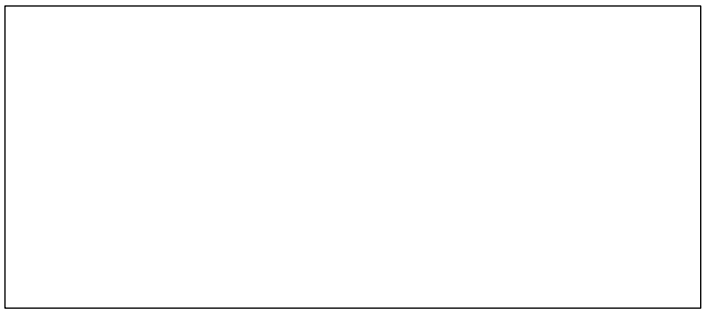

Forward planning with LGP

The forward planning was performed by expert planners with long-term experience as medical physics experts and two yearsô experience in GK therapy. The treatment planning system (TPS) used in this study is called Leksell GammaPlan® (version 11.3.1). With LGPôs internal inverse planning feature, the plans were generally optimized. For small-sized metastasis, only manual forward planning was used, mostly with one shot.

In general, the criteria for a good or acceptable plan are as follows: coverage of πϑω to ρϑππ, selectivity of πϑχ to ρϑππ, gradient index below σϑπ, beam-on time between ρπ ÍÉÎ and ρςπ ÍÉÎ. These may deviate in the individual case, depending on medical reasons such as the disease and the patient's medical history. The coverage, for instance, is of primary importance for single metastases, whereas the selectivity and the irradiation time are decisive factors for ANs and multiple metastases, respectively.

Inverse planning with IP

The cases were replanned through the inverse planning software IntuitivePlan® (version 1.0) after the export of the patient data from LGP. According to the departmental clinical protocol, the same dose constraints as for the LGP planning were set up. The optimization strategies (ñmaximize coverageò with the options ñfavor selectivityò or ñfavor BOTò and ñmaximize selectivityò) were specifically applied for the case or entity. To compare the elementary performance of the new algorithm with the present treatment (forward) planning method, neither the default parameters for each strategy were modified nor were any other sophisticated functions used in this study, such as 3D manipulation of the isodose surfaces. For patient treatment, the resulting shot configuration of IP plans generally needs to be exported back to LGP. It is necessary to adjust the optimized prescription dose (PD) from IP to integers, which consequently affects the dose distribution and plan quality metrics, but to a slight extent. Metastases were predominantly optimized according to the two strategies focusing on coverage, whereas the strategies ñmaximize selectivityò and ñmaximize coverage, favor selectivityò were mainly applied to benign entities, vascular and functional diseases.

Treatment plan evaluation

Both LGP and IP plans were preliminary and were based on non-stereotactic 3D MRI images with a simulated stereotactic frame. On the treatment day, the pre-plans were finally adjusted to the entity by co-registration with stereotactic tomography (CT).

To compare the planning results from both treatment planning methods or rather to assess the benefit for the target and healthy tissue, the following parameters were evaluated: coverage (C), selectivity (S), gradient index (GI), Paddick conformity index[6](PCI), efficiency index (EI), beam-on time (BOT), planning/computational time (t_{plan}), total set-up time (t_{total}), number of shots (N_{shots}), number of blocked sectors ($N_{blocked\ sectors}$), prescription isodose (PI), D_{min}, D_{mean}, D_{max}, and for risk assessment for brain tissue and OAR, $V_{10\ Gy}$, $V_{12\ Gy}$, $D_{skull\ mean}$, $D_{OAR\ transgression}$. The efficiency index proposed by Paddick[7] considers the ratio of integral dose inside and outside the target:

$$EI_{50\ \%} = \frac{\text{integral dose in target}}{\text{integral dose outside}} = \frac{\text{integral dose in } TV}{\text{integral dose in } PIV_{50\ \%}} = \frac{\int_{D_{min}}^{D_{max}} TV \cdot Dose}{\int_{D_{min}}^{D_{max}} PIV_{50\ \%} \cdot Dose}.$$

The parameters D_{min}, D_{mean}, and D_{max} describe the minimum, mean, and maximum dose, respectively. $PIV_{50\ \%}$ is the absolute volume of 50% of the PI. The efficiency index for multiple targets ($EI_{x\ Gy}$) fixes the problem of the gradient index for nearby targets that can overlap in $PIV_{50\ \%}$[7]:

$$EI_{x\ Gy} = \frac{\sum \text{integral dose in } TV_i}{\text{integral dose in } PIV_{x\ Gy}}.$$

The efficiency indices $EI_{50\ \%}$ and $EI_{x\ Gy}$ need to be extracted from the DVHs for LGP. The EI for single targets is automatically calculated by IntuitivePlan®.

One of the most relevant late toxicities occurring after stereotactic radiosurgery (SRS) is radionecrosis, which correlates with the volume of brain irradiated with 10 Gy ($V_{10\ Gy}$) or 12 Gy ($V_{12\ Gy}$)[8]. Likewise, we introduced the parameter $D_{OAR\ transgression}$, the difference between the maximum dose and dose constraint in the respective OAR (brainstem, cochlea, optic chiasma, pituitary, trigeminal nerve, vestibular apparatus, optical nerve). t_{total} describes

the sum of BOT and planning time. For the statistical ò-tests, the times per case instead of per TV have been considered for both the plan calculation time and the total time because IP only reported the total calculation time for the cases with multiple target volumes. Since the skull contouring was not feasible with the available Brainlab® ElementsÊ version, the mean brain dose is represented by the parameter Ò$_{skull\ mean}$.

Statistical analysis

Initially, we compared the IP strategies separately with LGP. Moreover, we investigated IP in terms of its applicability to malignant and benign diseases. To determine the statistical significance between the parameters of both planning methods, we conducted two-sided paired samples ò-tests[9,10] with a significance level of υ Þ (ǀ سي πΰπυ). The null hypothesis states that the mean values of LGP and IP do not differ (‘$_{LGP}$ سي ‘$_{IP}$).

With multiple testing, i.e., running various statistical tests on the same sample, the overall risk that at least one of the tests becomes falsely significant increases. To counteract alpha error accumulation, we used the conservative Bonferroni correction[9], which is why the significance level was adapted to ǀ^{z}سيǀ ϗè with è as the number of tests (ǀ^{z} سي πΰπυϗςπ سي πΰππςυ).

Because the sample size was too small for a statistical evaluation for both vascular and functional diseases, only the statistical calculations for the malignant and benign tumors were analyzed.

Results

Table 2 provides the summary statistics of the performed ὸ-tests dependent on the IP planning strategy, including p-values for each parameter and the mean difference (per TV) between the respective IP and LGP plan. Exemplary box plots in **Fig. 1** illustrate the distributions of the parameter selectivity.

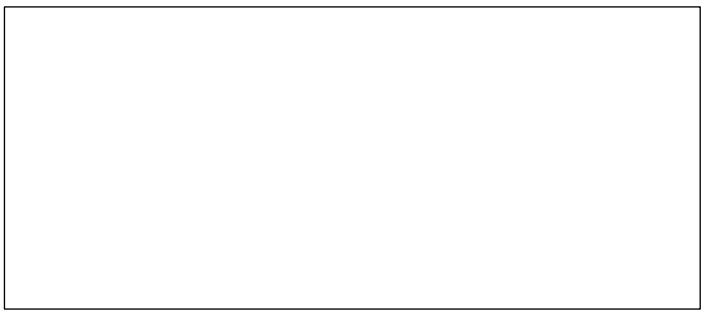

Figure 1 Anonymized for Review.

On average, we found significantly higher selectivity and PCI values for all available IP planning strategies with high significance (ى πϑππρ). These parameters improved remarkably for the selectivity strategies with a lower variance, as can be seen from the box plots in **Fig. 1**. This is additionally visualized in **Fig. 2** in which the inversely optimized isodose is closer to the tumor outline than for the conventional planning method.

Figure 2 Anonymized for Review.

The mean IP coverage values were barely distinguishable from the LGP coverage values, only inferior for the strategy prioritizing selectivity. The same applied to the mean GI values and their variance within the interquartile range, except for the strategy ñmaximize coverage, favor selectivityò. These results were reflected in an overall improved EI, or for the ñmaximum

coverage, favor BOTò strategy in an equal EI. Although there was a significantly lower $\dot{o}_{plan}$ per case for the strategies which prioritized selectivity, IP was slightly inferior to LGP in terms of BOT. These differences almost balanced out again in terms of $\dot{o}_{total}$. Furthermore, the isocenter number increased for all IP strategies. It should be noted that the optimized PI was either significantly below or above the manual adjusted, experience- and knowledge-based PI, independently of the IP strategy. The surrounding tissue, whose protection is characterized by ώ. ڏ or ώ ڏ[11,12], was exposed to approximately the same dose for both planning methods with similar variance, except for the strategy ñmaximize selectivityò

In contrast, the inverse planning yielded a high GI for the trigeminal neuralgia compared to LGP. Three more cases with trigeminal neuralgia were not included in the statistical testing, because they were not exportable from IP due to their high gradient index (حڍ ς) or their unsafe declared coverage. For all cases, the calculated PI was much higher than the PI set by the expert planner.

Table 2 Anonymized for Review.

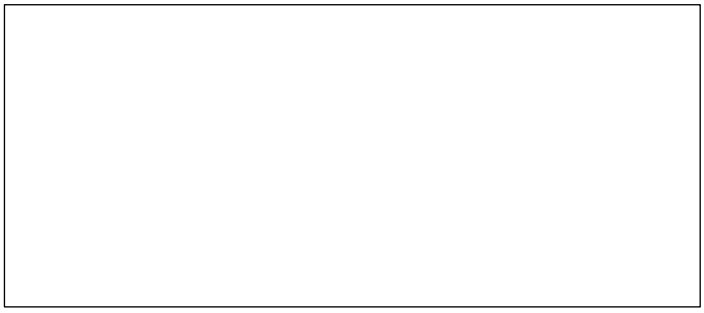

We additionally tested the performance of the inverse optimization for benign and malignant diseases separately (see **Fig. 3**, **Table B1**, **B2** and **Fig. A2**). **Fig. 4** specifically shows the

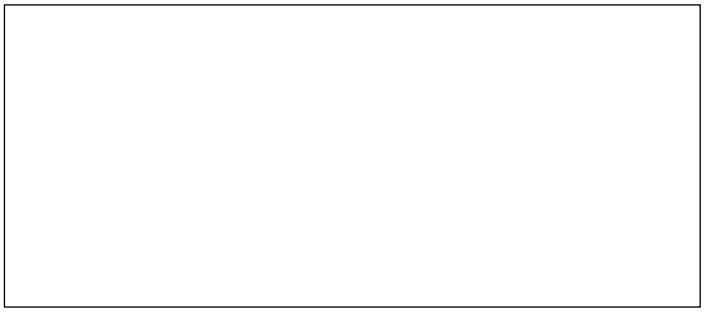

selectivity distribution for micrometastases with a volume حى ρ Ã Í σ.

Figure 3 Anonymized for Review.

Figure 4 Anonymized for Review.

Discussion

The results of our prospective trial with over 100 cases demonstrated that the inverse planning software IntuitivePlan® calculated comparable high-quality irradiation plans competing with the conventional forward planning. Significantly higher conformity values, shorter planning time, and better OAR sparing characterized the inverse calculated plans. The study demonstrated that the resulting IP plans with their quality metrics were highly dependent on the chosen strategy.

Compared to forward planning, the strategy ñmaximize selectivityò provided a significant improvement in conformity and a dose reduction in the brain as well as the respective OAR under reduced planning time. However, the dose gradients stayed the same and the BOT changed slightly. Even though the coverage was significantly lower for IP plans, this strategy was superior to the other two strategies used because the surrounding tissue and the OAR were exposed to a lower dose. Hence, we recommend ñmaximize selectivityò for benign cases–due to their irregular shape–that requires much experience and planning time. The "maximize coverage, favor selectivity" strategy obtained results similar to those of the selectivity-only optimizing strategy. Besides, the same TV coverage as for LGP and a steeper dose fall-off outside the TV were achieved compared to LGP. Substantiated by significantly higher è$_{shots}$, the BOT, however, was much longer, which is known to reduce the biologically effective dose[13] when treating malignant tumors.

To improve the coverage for the final plan, either the IP preset for the minimum selectivity could be changed before computing or the PI could be adapted after the optimization and the back-import into LGP. In most cases, we finally adapted the PI to achieve an even higher plan quality than the first-run IP pre-plans with the default optimization settings. Alternatively, the dosimetrist could manually adjust the isocenter configuration and the PI in the graphical user interface of IP.

A striking and contrasting result was the large difference in ὲ$_{blocked\ sectors}$. In general, manual planning includes more blocked sectors to spare radiosensitive tissue. Nevertheless, as the IP results reveal, there is no loss in the OAR protection without any blocked sectors.

The PI differed significantly for all strategies, which consequently influenced Ὀ$_{max}$ in the TV. Significantly higher isodoses simultaneously reduced the maximum doses (see strategy ñmaximum selectivityò). In GKRS, the PI for manual forward planning is usually the υπ Þ isodose because this is where the steepest dose gradients can be expected[14]. The effect of a higher or lower Ὀ$_{max}$ on the treatment outcome could not be confirmed so far so that a change of this is quite legitimate[15,16].

Upon closer examination of the benign diseases, IP was only better than LGP in GI and barely better in ὀ$_{plan}$ and Ὀ$_{OAR\ transgression}$. With respect to coverage, conformity, and sparing of surrounding tissue, IP was as good as LGP. The PI, by contrast, was comparatively higher for the same PD so that the Ὀ$_{max}$ in the target was lower. As a consequence, the reduced Ὀ$_{max}$ could decline the desired ablative effect of single-time irradiation of benign tumors. The dose-volume data of normal brain, a good predictor of radionecrosis, was approximately the same for both planning methods, but with higher brain protection for the ñmaximum selectivityò strategy. Further reduction would still be desirable. According to Blonigen et al[8], the risk to develop radionecrosis would be already στ Þ for measured values of φϋτ ﻁ ρτϋυ cm^3 and τϋψ ﻁ ρπϋψ cm^3 in the ώ ِ ِ ِ and ώ . ِ ِ distribution, respectively.

The so-called ñone-shot plansò, which were created manually for multiple metastases and micrometastases, did show advantages compared to IP plans. Although the target conformity was much higher for IP plans optimized with ñmaximum coverage, favor selectivityò than that for LGP, the most important goal for these malignant cases is the TV coverage, followed by a short BOT for patients with a poor state of health. Since the strategy ñmaximum coverage, favor selectivityò primarily focuses on conformity, the BOT is considerably increased. For multiple metastases, the strategy ñmaximize coverage, favor BOTò seems to be most suitable but often not preferable to the standard manual method in which a single isocenter with the

smallest possible collimator is used. For micrometastases, the surrounding brain tissue receives little dose, even with high coverage. Thus, a lower selectivity of manual single-shot plans would be less clinically relevant. More selective plans, generated by IP as default, would lead to an increase in BOT due to higher ὲ$_{shots}$.

Previous work by Régis[17] and Paddick[18] focused primarily on ANs and AVMs that require maximum selectivity. In our trial, however, the small sample size of AVMs hampered meaningful conclusions. In contrast to these previous studies [17,18], the IP strategy was not the same for all cases and varied depending on the entity. The significantly higher ὲ$_{shots}$ of IP plans, which is contrary to usual expert planning, is in line with Paddick and Régis[17,18]. Yet, we could not verify the strong influence of ὲ$_{shots}$ on the BOT. The non-superiority of the GI (except for the strategy ῥmaximize coverage, favor selectivityὸ) is also consistent with former studies. Our study does not (entirely) confirm previous results regarding selectivity and PCI, because these studies achieved higher conformity values for their manual plans than our manual pre-plans (΅Ὑ سي πϑωρπ ى πϑπχτ, PCI سي πϑψωψ ى πϑπχφ in R®gisô study; ΅Ὑ سي πϑψυφ, PCI سي πϑψςτ in Paddickὸs study). Paddick et al. assumed a positive correlation between BOT and PCI[18]. We proved that these parameters correlate depending on the planning method (ìئïäځځحح سي πϑπωψ, ìئïäځځحح سي πϑσς, ìئïäځځحح سيطπϑπσ for ῥmaximize coverage, favor selectivityὸ, ῥmaximize coverage, favor BOTὸ, ῥmaximize selectivityὸ). ANs represent one of the most challenging indications in SRS, even though the GK was originally developed for such purposes in 1969[19,20]. Our study included 21 AN cases for which 20 IP plans were preferred with the strategy ῥmaximize selectivityὸ due to comparatively higher selectivity (IP: πϑψω ى πϑπφ vs. LGP: πϑχτ ى πϑρτ) despite lower coverage (IP: πϑωφ ى πϑπτ vs. LGP: πϑωψχ ى πϑππχ). Both previous studies did not verify the superiority of IP in OAR and brain sparing. Especially for the strategy ῥmaximize selectivityὸ, our findings contrast with these results. The underlying reason is that in both studies[17,18], no pre-plans but highly optimized forward plans were used for the comparison with IP.

The planner's assessment and experience considerably influence the resulting plans, especially for GK centers with less experienced in stereotaxis personnel. Moreover, further improvements in the clinically acceptable LGP pre-plans (e.g., higher conformity) were certainly possible but had to be weighed against the planning time. As noted, the compared plans were preliminary. Staffed with more dosimetrists and equipped with a stereotactic planning MRI allowing for planning directly on stereotactic MRI images, many GK facilities routinely do not use pre-planning. Our methodology is therefore more suitable for smaller institutions. If pre-planning, the planner can spend more time on a specific case, compare different plan versions, and then select the optimal plan, which removes the time pressure on the treatment day as the patient is waiting with the frame attached. For teams with medium experience in stereotaxis, such an algorithm provides a plan alternative or basis.

Unlike non-stereotactic TPSs, TPS in GKRS did not include a global algorithm. IP was the first available third-party algorithm for GK. A comparable algorithm Leksell Gamma Knife® Lightning was offered only later by the GK manufacturer. According to our information, there is no direct relation between the two algorithms[21]. The algorithm used here is freely available now and it has been and is still used in other, non-medical areas (e.g., in the planning of power supply networks) and for scientific purposes. Although the implementation in a GK-plan-compatible software is longer available for purchase, its fundamental aspects of the general usage of an optimization algorithm can nevertheless be transferred. First, inverse planning can save much time in planning and make full use of the GK device. Second, if one has the possibility to select different objectives/strategies, several optimized plans can be compared more easily to find the most suitable plan for the respective disease, its stage, and localization. Further possibilities for manual post-plan adaptation or for modification of default optimization settings, as provided by IP, allow for taking the anamnesis into account.

Conclusions

The inverse planning algorithm achieved clinically acceptable pre-plans for all planning strategies within a reasonable time and with at least equal or superior quality compared to LGP. Therefore, the algorithm proves beneficial in clinical routine, especially for smaller GK facilities with less experienced planners. Our findings suggest that inverse planning is generally appropriate for complex-shaped tumors and that forward planning, by contrast, is suitable for trigeminal neuralgia or micrometastases.

Supplementary Materials

Further box plots of the parameters investigated as well as the analysis of benign and malign tumors can be found in the online version

Declaration of interests

☐The authors declare that they have no known competing financial interests or personal relationships that could have appeared to influence the work reported in this paper.
☒The authors declare the following financial interests/personal relationships which may be considered as potential competing interests:

Jan Bostroem reports equipment, drugs, or supplies was provided by Intuitive Therapeutics.

References

1. Leksell L. The stereotaxic method and radiosurgery of the brain. *Acta Chir Scand*. 1951;102(4):316-319.

2. Hamilton T, Lunsford LD. Worldwide variance in the potential utilization of Gamma Knife radiosurgery. *J Neurosurg*. 2016;125(Supplement_1):160-165. doi:10.3171/2016.7.GKS161425

3. Vergalasova I, Liu H, Alonso-Basanta M, et al. Multi-Institutional Dosimetric Evaluation of Modern Day Stereotactic Radiosurgery (SRS) Treatment Options for Multiple Brain Metastases. *Front Oncol*. 2019;9:483. doi:10.3389/fonc.2019.00483

4. Liġ§k R. *Gamma Knife Radiosurgery*. Nova Science Publishers; 2013.

5. Levivier M, Carrillo RE, Charrier R, Martin A, Thiran JP. A real-time optimal inverse planning for Gamma Knife radiosurgery by convex optimization: description of the system and first dosimetry data. *J Neurosurg*. 2018;129(Suppl1):111-117. doi:10.3171/2018.7.GKS181572

6. Paddick I, Lippitz B. A simple dose gradient measurement tool to complement the conformity index. *J Neurosurg*. 2006;105(Supplement):194-201. doi:10.3171/sup.2006.105.7.194

7. Dimitriadis A, Paddick I. A novel index for assessing treatment plan quality in stereotactic radiosurgery. *J Neurosurg*. 2018;129(Suppl1):118-124. doi:10.3171/2018.7.GKS18694

8. Blonigen BJ, Steinmetz RD, Levin L, Lamba MA, Warnick RE, Breneman JC. Irradiated Volume as a Predictor of Brain Radionecrosis After Linear Accelerator Stereotactic Radiosurgery. *Int J Radiat Oncol Biol Phys*. 2010;77(4):996-1001. doi:10.1016/j.ijrobp.2009.06.006

9. Rasch D, Schott D. *Mathematical Statistics*. John Wiley & Sons; 2018.

10. Riffenburgh RH, Gillen DL, eds. *Statistics in Medicine*. In: 4th ed. Academic Press; 2020:ix-xvi. doi:10.1016/B978-0-12-815328-4.00031-0

11. Hellerbach A, Luyken K, Hoevels M, et al. Radiotoxicity in robotic radiosurgery: proposing a new quality index for optimizing the treatment planning of brain metastases. *Radiat Oncol*. 2017;12(1):1-9. doi:10.1186/s13014-017-0867-z

12. G M, E C, G L, et al. Stereotactic radiosurgery for brain metastases: analysis of outcome and risk of brain radionecrosis. *Radiat Oncol Lond Engl*. 2011;6. doi:10.1186/1748-717X-6-48

13. Millar WT, Hopewell JW, Paddick I, et al. The role of the concept of biologically effective dose (BED) in treatment planning in radiosurgery. *Phys Med*. 2015;31(6):627-633. doi:10.1016/j.ejmp.2015.04.008

14. *Robotergeführte Radiochirurgie: Cranielle und Spinale Indikationen*. De Gruyter; 2020. doi:10.1515/9783110540598

15. Nakamura JL, Verhey LJ, Smith V, et al. Dose conformity of gamma knife radiosurgery and risk factors for complications. *Int J Radiat Oncol*. 2001;51(5):1313-1319. doi:10.1016/S0360-3016(01)01757-6

16. Sneed PK, Mendez J, Vemer-van den Hoek JGM, et al. Adverse radiation effect after stereotactic radiosurgery for brain metastases: incidence, time course, and risk factors. *J Neurosurg*. 2015;123(2):373-386. doi:10.3171/2014.10.JNS141610

17. Régis J, Hamdi H, Loundou A, et al. Clinical evaluation of a real-time inverse planning for Gamma Knife radiosurgery by convex optimization: a prospective comparative trial in a series of vestibular schwannoma patients. *Acta Neurochir (Wien)*. 2021;163(4):981-989. doi:10.1007/s00701-020-04695-x

18. Paddick I, Grishchuk D, Dimitriadis A. IntuitivePlan inverse planning performance evaluation for Gamma Knife radiosurgery of AVMs. *J Appl Clin Med Phys*. 2020;21(9):90-95. doi:https://doi.org/10.1002/acm2.12973

19. Hirsch A, Norén G, Anderson H. Audiologic findings after stereotactic radiosurgery in nine cases of acoustic neurinomas. *Acta Otolaryngol (Stockh)*. 1979;88(3-4):155-160. doi:10.3109/00016487909137155

20. Leksell L. Stereotactic radiosurgery. *J Neurol Neurosurg Psychiatry*. 1983;46(9):797-803.

21. Sjölund J, Riad S, Hennix M, Nordström H. A linear programming approach to inverse planning in Gamma Knife radiosurgery. *Med Phys*. 2019;46(4):1533-1544. doi:10.1002/mp.13440

Figure captions

Figure 1 Box plots for parameter selectivity dependent on the IP strategy including all cases.

i) "maximize coverage, favor selectivity", ii) "maximize coverage, favor BOT", iii) "maximize selectivity".

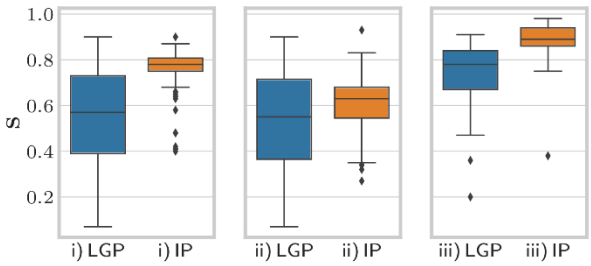

Fig. 1

Figure 2 Horizontal T2-weighted MRIs demonstrating the comparison between the IP and LGP plan for a representative AN case adjacent to the brainstem.

Left: LGP plan with ő سي πϐωω and ‴ϒ سي πϐψτ. Right: IP plan with ő سي πϐωψ and ‴ϒ سي πϐωτ. The red-black shaded area represents the intersection of the TV (red) and the 12-Gy prescription isodose (yellow). *Abbreviation:* PIV = prescription isodose volume.

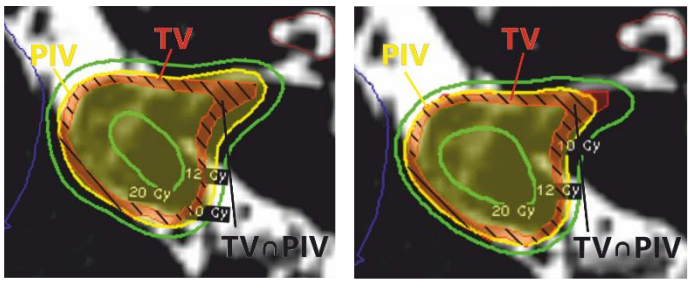

Fig. 2

Figure 3 Comparison of benign and malignant entities regarding selectivity.

Top: box plots for benign entities depending on the strategy i)/ii)/iii) (same notation as in Fig. 1). Bottom: box plots for malignant entities.

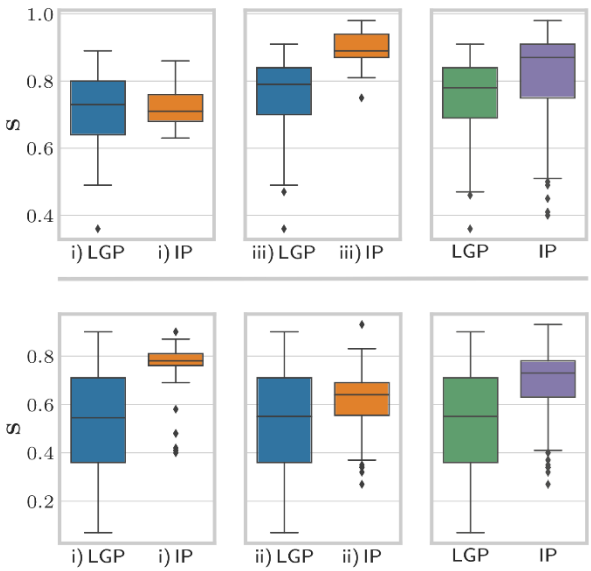

Fig. 3

Figure 4 Results for micrometastases regarding selectivity.

Box plots for micrometastases (with ρ طي Í Í safety margin) depending on the strategy i) and ii) (same notation as in Fig.1).

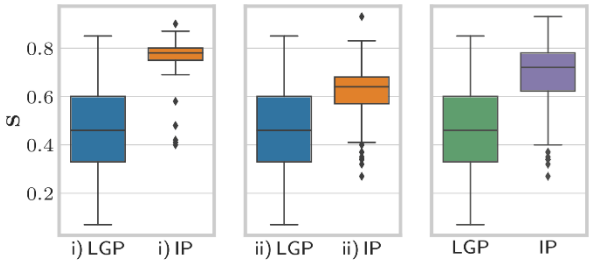

Fig. 4

Index of Abbreviations

AN	acoustic neuroma
AVM	arteriovenous malformation
BOT	beam-on time
CT	computed tomography
DVH	dose-volume histogram
EI	efficiency index
GI	gradient index
GK	Gamma Knife®
GKRS	Gamma Knife radiosurgery
IP	inverse planning (with IntuitivePlan®)
LGP	Leksell GammaPlan®
MRI	magnetic resonance imaging
OAR	organ at risk
PCI	Paddick conformity index
PD	prescription dose
PI	prescription isodose
SRS	stereotactic radiosurgery
TPS	treatment planning system
TV	target volume

Table 1 Patient demographics

	ĩ	ῆ꒐ɛ꒐Þ **in Ã Í ᵞ**	ΈȀ꒐ɛ꒐Þ **in 'Ù**
TVs	ςσπ	πȣυυππ	ρψȣπ
Malign tumors	ρφτ	πȣσφςυ	ςπȣπ
Benign tumors	φρ	ρȣτχψπ	ρτȣπ
Vascular diseases	τ	ρȣσφυυ	ρφȣπ
Functional diseases	ρ	πȣπρρπ	ωπȣπ

Abbrevations: TV = target volume; n = number of the TVs; ώ꒐ی꒐Þ = *median target volume;* ΰ'Ο꒐ی꒐Þ = median prescription dose for forward planning.

Table 2 Results with IP plans for the default single run depending on the strategy

Parameter	Strategy	LGP ᾱ عى "ı	IP ᾱ عى "ı	ᾱ–ᾱ عى "ı	p (ط سي ٤ὸ٤٩)	Significance
PI in %	i)	υρ عى φ	τψ عى ω	ςὸω عى ρρ	πὸπππσzzz	yes
	ii)	υρ عى χ	υφ عى ρς	طτὸχ عى ρσ	ςὸτω z ρπ٩٤ zzz	yes
	iii)	υπὸυ عى ςὸτ	υτ عى ψ	طσὸτ عى ψ	πὸπππυzzz	yes
C	i)	πὸωωυ عى πὸππω	πὸωωυ عى πὸπρτ	πὸπππς عى πὸπρχ	πὸψωυς	no
	ii)	πὸωωφ عى πὸππψ	πὸωωψ عى πὸπρτ	طπὸππςφ عى πὸπρφ	πὸπσσωz	yes
	iii)	πὸωψτ عى πὸππω	πὸωφχ عى πὸπςψ	πὸπρχ عى πὸπσ	σὸωρ z ρπ٩٣ zzz	yes
S	i)	πὸυυ عى πὸςς	πὸχφ عى πὸπψ	طπὸςρυ عى πὸςς	υὸως z ρπ٩١ي zzz	yes
	ii)	πὸυτ عى πὸςρ	πὸφρ عى πὸρς	طπὸπχρ عى πὸςυ	πὸπππςzzz	yes
	iii)	πὸχτ عى πὸρτ	πὸψω عى πὸπω	طπὸρττ عى πὸρ	ρὸτψ z ρπ٩٠٥ zzz	yes
GI	i)	σὸρ عى πὸτ	σὸπ عى πὸυ	πὸρψ عى πὸφ	πὸπππςzzz	yes
	ii)	σὸρ عى πὸυ	σὸρ عى πὸυ	πὸπσ عى πὸφ	πὸυτχς	no
	iii)	σὸπς عى πὸςω	σὸπ عى πὸφ	πὸππ عى πὸυ	πὸωψχχ	no
PCI	i)	πὸυυ عى πὸςρ	πὸχφ عى πὸπψ	طπὸςρτ عى πὸςρ	ψὸχς z ρπ٩١٠ zzz	yes
	ii)	πὸυσ عى πὸςρ	πὸφρ عى πὸρς	طπὸπχτ عى πὸςυ	πὸπππρzzz	yes
	iii)	πὸχσ عى πὸρτ	πὸψφ عى πὸπω	طπὸρςψ عى πὸπω	σὸπσ z ρπ٩٠٥ zzz	yes
EI in Þ	i)	τπ عى ρσ	υπ عى ω	ςὸσ عى φ	ρὸχτ z ρπ٩٠ي zzz	yes
	ii)	σω عى ρρ	σχ عى ρπ	ρὸυ عى ρς	πὸσωρρ	no
	iii)	τς عى ρσ	49عىρσ	طφὸυ عى τ	τὸχσ z ρπ٩٠٣ zzz	yes
ὸplan per case in ά⃝è	i)	χ عى χ	τ عى υ	ςὸσ عى φ	πὸππςρzz	yes
	ii)	χ عى ψ	τ عى υ	ρὸψ عى ρς	πὸπφυτ	no
	iii)	ω عى υ	σὸω عى ςὸψ	υὸσ عى υ	σὸττ z ρπ٩٠٠ zzz	yes
BOT in ά⃝è	i)	ςυ عى ρσ	συ عى ρφ	طρπ عى ρυ	ςὸχψ z ρπ٩٠٥ zzz	yes
	ii)	ςσ عى ρς	ςς عى ρπ	ρὸψ عى ρς	πὸπτππz	yes
	iii)	σω عى ρυ	τς عى ρψ	طσὸσ عى ρσ	πὸπσωρz	yes
ὸtotal per case in ά⃝è	i)	χπ عى υπ	ωπ عى χπ	طςσ عى υπ	τὸρφ z ρπ٩٣ zzz	yes
	ii)	χπ عى φπ	φπ عى φπ	τ عى τπ	πὸτρωτ	no
	iii)	υς عى ςρ	υρ عى ςτ	ρὸπ عى ρυ	πὸυωυω	no
èshots	i)	τ عى φ	ρσ عى ρπ	طω عى ω	ψὸρω z ρπ٩١٠ zzz	yes
	ii)	τ عى υ	ρπ عى ψ	طφὸφ عى χ	υὸυψ z ρπ٩١ي zzz	yes
	iii)	ρς عى χ	ςω عى ρυ	طρφὸς عى ρρ	ρὸςχ z ρπ٩٠٥ zzz	yes
èblocked sectors	i)	σ عى φ	υ عى ψ	طςὸσ عى ρπ	πὸπππχzzz	yes
	ii)	ς عى υ	ς عى υ	πὸσ عى χ	πὸτωςχ	no
	iii)	ρπ عى ψ	σ عى χ	χὸρ عى ρρ	ρὸφχ z ρπ٩٤ zzz	yes
ώₒ.ₑₐ in ώ̃ά'	i)	τ عى ρπ	σ عى υ	ρὸρ عى ω	πὸπωπφ	no
	ii)	τ عى ρπ	τ عى φ	πὸσ عى ω	πὸφωφτ	no
	iii)	τ عى φ	τ عى υ	πὸυφ عى πὸψ	ρὸςτ z ρπ٩٥ zzz	yes
ώₒيₑₐ in ώ̃ά'	i)	υ عى φ	τ عى φ	πὸχτ عى τ	πὸππυπzz	yes
	ii)	υ عى χ	υ عى ψ	طπὸτσ عى τ	πὸρυτφ	no
	iii)	φ عى χ	υ عى φ	πὸψψ عى ρὸς	ψὸψρ z ρπ٩٤ zzz	yes
Ὀskull mean in 'Ù	i)	πὸτ عى πὸτ	πὸτ عى πὸτ	πὸπςψ عى πὸρφ	πὸρφυφ	no
	ii)	πὸυ عى πὸτ	πὸυ عى πὸυ	طπὸπυπ عى πὸρυ	πὸπςτυz	yes
	iii)	πὸςχ عى πὸςς	πὸσ عى πὸυ	طπὸπσ عى πὸτ	πὸυχυχ	no
Ὀmin in 'Ù	i)	ρχ عى υ	ρχὸχ عى ςὸχ	طπὸφ عى υ	πὸπχωφ	no
	ii)	ρψ عى υ	ρωὸσ عى σὸπ	طρὸχ عى υ	ρὸτυ z ρπ٩٣ zzz	yes
	iii)	ρρ عى ψ	ρς عى χ	طπὸυ عى ςὸυ	πὸρρυω	no
Ὀmean in 'Ù	i)	ςψ عى χ	ςψ عى τ	πὸχ عى φ	πὸρπρς	no
	ii)	ςω عى φ	ςχ عى υ	ςὸς عى φ	ρὸψ z ρπ٩٤ zzz	yes
	iii)	ςπ عى ω	ρω عى ψ	ρὸς عى ςὸσ	πὸπππσ	yes
Ὀmax in 'Ù	i)	σχ عى φ	τπ عى ω	طσὸσ عى ω	υὸυχ z ρπ٩٥ zzz	yes
	ii)	σχ عى υ	συ عى ω	ςὸω عى10	υὸυς z ρπ٩٣ zzz	yes
	iii)	ςψ عى ω	27عىψ	ρὸσ عى υ	πὸπςρρz	yes
ὈOAR transgression in 'Ù	i)	طρ عى φ	طς عى υ	ρὸσ عى ςὸπ	πὸππρυzz	yes
	ii)	ς عى υ	طρὸπ عى ςὸτ	ςὸχ عى ςὸυ	πὸπσωψz	yes
	iii)	π عى υ	طς عى υ	ρὸυς عى ρὸχ	υὸυρτ z ρπ٩٠١ zzz	yes

Abbrevations: i) "maximize coverage, favor selectivity"; ii) "maximize coverage, favor BOT"; iii) "maximize selectivity"; ᾱ = mean value of the respective parameter for LGP; ᾱ = mean value for IP; í = corrected sample standard deviation.

† EI includes –٣ي Þ and ῍Ὀ–ₒ. *Gy*.

* ἡ حى πὸπυ; ** ἡ حى πὸπρ; *** ἡ حى πὸππρ.
Marked in red are those rows that have a p-value just below | سي πὸπυ but above | z. Values for ὈOAR transgression should be interpreted with caution because OARs did not exist for every case (e.g., metastases). For the strategies i), ii) and iii) ςψ, χ, and ψχ OARs are counted, respectively. Notice the different sample sizes for each strategy and every parameter.